Hydroxyl Radical-Mediated Novel Modification of Peptides: N-Terminal Cyclization through the Formation of α-Ketoamide

ARTICLE *in* CHEMICAL RESEARCH IN TOXICOLOGY · NOVEMBER 2014

Impact Factor: 3.53 · DOI: 10.1021/tx500332y · Source: PubMed

Chemical Research in Toxicology

Article

pubs.acs.org/crt

Hydroxyl Radical-Mediated Novel Modification of Peptides: N-Terminal Cyclization through the Formation of α-Ketoamide

Seon Hwa Lee,* Hyunsook Kyung, Ryo Yokota, Takaaki Goto, and Tomoyuki Oe*

Department of Bio-analytical Chemistry, Graduate School of Pharmaceutical Sciences, Tohoku University, Sendai 980-8578, Japan

Supporting Information

ABSTRACT: The hydroxyl radical-mediated oxidation of peptides and proteins constitutes a large group of post-translational modifications that can result in structural and functional changes. These oxidations can lead to hydroxylation, sulfoxidation, or carbonylation of certain amino acid residues and cleavage of peptide bonds. In addition, hydroxyl radicals can convert the N-terminus of peptides to an α-ketoamide via abstraction of the N-terminal α-hydrogen and hydrolysis of the ketimine intermediate. In the present study, we identified N-terminal cyclization as a novel modification mediated by a hydroxyl radical. The reaction of angiotensin (Ang) II (DRVYIHPF) and the hydroxyl radical generated by the Cu(II)/ascorbic acid (AA) system or UV/hydrogen peroxide system produced N-terminal cyclized-Ang II (Ang C) and pyruvamide-Ang II (Ang P, $CH_3COCONH$-RVYIHPF). The structure of Ang C was confirmed by mass spectrometry and comparison to an authentic standard. The subsequent incubation of isolated Ang P in the presence of Cu(II)/AA revealed that Ang P was the direct precursor of Ang C. The proposed mechanism involves the formation of a nitrogen-centered (aminyl) radical, which cyclizes to form a five-membered ring containing the alkoxy radical. The subsequent β-scission reaction of the alkoxyl radical results in the cleavage of the terminal CH_3CO group. The initial aminyl radical can be stabilized by chelation to the Cu(II) ions. The affinity of Ang C toward the Ang II type 1 receptor was significantly lower than that of Ang II or Ang P. Ang C was not further metabolized by aminopeptidase A, which converts Ang II to Ang III. Hydroxyl radical-mediated N-terminal cyclization was also observed in other Ang peptides containing N-terminal alanine, arginine, valine, and amyloid β 1−11 (DAEFRHDSGYE).

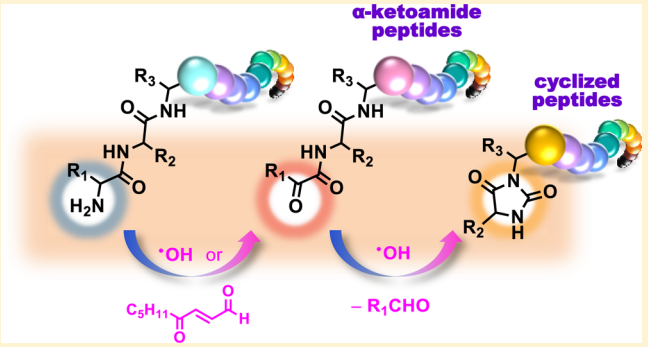

INTRODUCTION

Free radicals are any species (atom, molecule, or ion) that have an unpaired electron. They can be generated in biological systems by endogenous processes (e.g., metabolic pathways and enzymes) or by exposure to external stimuli (e.g., γ-radiation and UV light).[1] Reactive oxygen species (ROS) are oxygen-containing reactive molecules. ROS include oxygen radicals such as superoxide ($O_2^{\bullet-}$) and hydroxyl radicals ($HO^{\bullet}$), and nonradical oxidants such as hydrogen peroxide (H_2O_2) and hypochlorous acid (HOCl), which can be easily converted to radicals.[1,2] ROS are constantly formed in vivo as byproducts of various metabolic processes, including normal mitochondrial aerobic respiration, phagocytosis of bacteria or virus-containing cells, and peroxisomal-mediated degradation of fatty acids.[3] There are also enzymatic sources of ROS that have specific roles in physiology such as cytochrome P450,[3,4] xanthine oxidase, and NADPH oxidases.[5] Under physiological conditions, ROS can regulate intracellular signaling through the modification of Cys residues in redox-sensitive proteins[6] and can be protective when they are stimulated by macrophages as an immune response to bacterial infection.[7] In general, ROS can be detoxified by the endogenous defense systems. These defenses include small molecules (e.g., ascorbic acid and α-tocopherol) that react with radicals to generate less reactive species and enzymes that remove nonradical oxidants (e.g., catalase and glutathione peroxidase) and that directly scavenge radicals (e.g., superoxide dismutase).[1,3] There are also enzymes that repair ROS-mediated damage (e.g., methionine sulfoxide reductase and disulfide reductase).[1] However, alterations in the balance between the formation of ROS, their removal, and damage repair cause oxidative damage, which is often referred to as oxidative stress. Increased ROS production has been associated with a number of inflammatory and age-related degenerative diseases.[2,3]

The hydroxyl radical is among the most reactive ROS and can interact with almost every type of molecule found in living cells, including DNA, lipids, carbohydrates, and proteins.[2,8−10] Hydroxyl radicals can oxidize amino acids, peptides, and proteins through a variety of reactions, including hydrogen abstraction, addition, fragmentation, and rearrangement.[10,11] Hydrogen abstraction is the main process for most free amino acids containing an aliphatic side chain.[10,12] It occurs at sites far from the deactivating protonated α-amino group, mainly

Received: August 18, 2014
Published: November 25, 2014

   dx.doi.org/10.1021/tx500332y | Chem. Res. Toxicol. 2015, 28, 59−70

resulting in the formation of side chain radicals. The resulting radicals can be stabilized by electron delocalizing groups. Thus, the preferential sites for hydrogen abstraction are adjacent to hydroxyl groups in Ser and Thr, carboxyl and amide groups in Asp, Glu, Asn, and Gln, and the guanidino group in Arg.[12] Aromatic amino acids, such as Phe, Tyr, Trp, and His, undergo radical addition to yield various hydroxylated and quinone/carbonyl species.[10,12] The sulfur atoms in Met and Cys are major oxidation targets of both radical and nonradical oxidants. Radical-mediated oxidation of Met results in sulfoxide formation via an addition reaction.[13] In Cys, the radicals participate in rapid hydrogen abstraction from the thiol group to yield thiyl radicals ($RS^{\bullet}$), which can dimerize to give disulfide species[14] or can be oxidized further to produce sulfenic, sulfinic, and sulfonic acids via the formation of a thiyl peroxyl radical.[10] In contrast to free amino acids, radicals can cause significant levels of backbone oxidation on peptides and proteins because the α-carbon radical formed through hydrogen abstraction is stabilized by both the neighboring amide and carbonyl groups.[11] The resulting carbon-centered radical is rapidly converted to the peroxyl radical in the presence of O_2. Subsequently generated alkyl peroxides and alkoxyl radicals can then undergo cleavage by either the α-amidation or the diamide pathways.[15] The extent of backbone versus side chain oxidation depends on the accessibility of each site and the secondary and tertiary structures of the peptide or protein. Radicals form predominantly on side chains in larger peptides and proteins because of the steric hindrance of the main chain α-carbon.[10,11] Site-specific oxidation can occur when metal ions are used to generate radicals. Metal ions, such as Fe and Cu, can undergo complexation with or bind to particular sites in peptides and proteins. The generated hydroxyl radicals can react with amino acids in the vicinity, inducing site-selective peptide and protein damage.[15,16] Free radical-mediated oxidation of backbone and amino acid residues results in structural and functional changes in peptides and proteins.[16−18]

4-Oxo-2(*E*)-nonenal (ONE) is a major bifunctional electrophile derived from lipid hydroperoxides, and it can modify DNA,[19,20] RNA,[21] peptides and proteins,[22−24] and GSH[25] through adduct formation. In addition, ONE can mediate N-terminal epimerization[26] and introduce an α-ketoamide moiety at the N-terminus of peptides.[27,28] Hydroxyl radical can also convert the N-terminus of peptides to an α-ketoamide via abstraction of the N-terminal α-hydrogen and hydrolysis of the ketimine intermediate.[28] As an example, pyruvamide-angiotensin II (Ang P, $CH_3COCONH$-RVYIHPF) was generated from angiotensin II (Ang II, DRVYIHPF) by a ONE- or a hydroxyl radical-mediated reaction. Ang P has a much lower affinity than Ang II for Ang II type 1 (AT_1) receptors, indicating that the N-terminal pyruvamide group significantly inhibits the binding of Ang P to the AT_1 receptor.[29] N-Terminal α-ketoamide was further converted to the D- and L-amino acids by nonenzymatic transamination in the presence of pyridoxamine (PM).[28] In the present study, we describe a novel hydroxyl radical-mediated N-terminal cyclization via α-ketoamide formation. Liquid chromatography (LC) and mass spectrometry (MS) were used to characterize the modification, and various bioactive peptides were employed to confirm the N-terminal cyclization.

MATERIALS AND METHODS

Materials. Human Ang I (DRVYIHPFHL), Ang II (DRVYIHPF), Ang III (RVYIHPF), Ang IV (VYIHPF), and amyloid β 1−11 ($A\beta_{1-11}$, DAEFRHDSGYE) were obtained from the Peptide Institute, Inc. (Osaka, Japan). Ang A (ARVYIHPF), Ang P ($CH_3COCONH$-RVYIHPF), and N-terminal cyclized-Ang II (Ang C) were synthesized and supplied by Toray Research Center, Inc. (Tokyo, Japan). [$^{13}C_5$,$^{15}N_1$-Pro^7]-Ang II was obtained from Scrum, Inc. (Tokyo, Japan). ONE was purchased from Cayman Chemical Co. (Ann Arbor, MI). Recombinant human aminopeptidase A (APA) was purchased from R&D Systems, Inc. (Minneapolis, MN, USA). Copper(II) sulfate pentahydrate ($CuSO_4 \cdot 5H_2O$), zinc(II) sulfate heptahydrate ($ZnSO_4 \cdot 7H_2O$), iron(II) sulfate heptahydrate ($FeSO_4 \cdot 7H_2O$), iron(III) chloride hexahydrate ($FeCl_3 \cdot 6H_2O$), calcium chloride ($CaCl_2$), α-cyano-4-hydroxycinamic acid (CHCA), and ammonium acetate were obtained from Wako Pure Chemical Industries, Ltd. (Osaka, Japan). L-Ascorbic acid (AA) and tris(hydroxymethyl)aminomethane hydrochloride (Tris) were purchased from Sigma-Aldrich Inc. (St. Louis, MO). Formic acid, trifluoroacetic acid, hydrochloric acid, sodium chloride, and hydrogen peroxide were purchased from Nacalai Tesque, Inc. (Kyoto, Japan). Chelex-100 chelating ion-exchange resin (100−200 mesh size) was purchased from Bio-Rad Laboratories (Hercules, CA). LC grade acetonitrile and ethanol were obtained from Kanto Chemical Co. Inc. (Tokyo, Japan). Ultrapure water was obtained from a Milli-Q Integral 10 system (EMD Millipore, Billerica, MA) equipped with a 0.22 μm membrane cartridge. Oasis HLB cartridges were obtained from Waters Corp. (Milford, MA). All peptides, transition metal ions, and AA were dissolved in 50 mM Chelex-treated phosphate buffer (PB), and the final concentrations used in each experiment are described unless otherwise stated.

Infrared Spectroscopy. Fourier transform (FT)-infrared (IR) spectra were obtained on an FT/IR-400Plus spectrometer (JASCO Co., Tokyo, Japan) with an ATR PRO410-S single reflection/attenuated total reflection (ATR) accessory. A solid sample (approximately 0.1 mg) was applied on the ATR prism and then measured directly. The operating conditions for FT/IR-400Plus and ATR PRO410-S were as follows: method, ATR spectroscopy/single reflection; light source, high-intensity ceramic; detector, triglycine sulfate; angle of incidence, 45°; prism, ZnSe; optical system, single beam; range, 4000−650 cm^{-1}; integration, 16 times; resolution, 4 cm^{-1}; apodization, cosine; scanning speed, 2 mm/sec; and data processing, Spectra Manager, version 1.09.00 (JASCO Co.).

Liquid Chromatography. Chromatographies for LC/electrospray ionization (ESI)-MS analyses were carried out on an Agilent 1100 LC system (Agilent Technologies, Inc., Santa Clara, CA) equipped with a G1312A binary pump, a G1329A ALS autosampler, and a G1379A degasser at ambient temperature using LC gradient systems 1−4. Chromatography for the isolation of Ang P and Ang C was carried out on a Nanospace SI-1 semimicrocolumn LC system (Shiseido Co. Ltd., Tokyo, Japan) equipped with a UV detector using gradient system 5. All separations were performed on a Jupiter C18 column (150 × 2.0 mm i.d., 5 μm, 300 Å; Phenomenex, Torrance, CA) with a flow rate of 0.2 mL/min at ambient temperatures. For LC systems 1 and 3, solvent A was water/acetonitrile (98:2, v/v) containing 0.2% formic acid, and solvent B was acetonitrile/water (98:2, v/v) containing 0.2% formic acid. The linear gradient for LC system 1 was as follows: 10% B at 0 min, 70% B at 30 min, 95% B at 31 min, 95% B at 34 min, 10% B at 35 min, and 10% B at 50 min. The linear gradient for LC system 3 was as follows: 10% B at 0 min, 80% B at 30 min, 95% B at 31 min, 95% B at 34 min, 10% B at 35 min, and 10% B at 50 min. For LC system 2, solvent A was water/acetonitrile (98:2, v/v) containing 0.1% formic acid, and solvent B was acetonitrile/water (70:30, v/v) containing 0.1% formic acid. The linear gradient was as follows: 20% B at 0 min, 20% B at 2 min, 31% B at 17 min, 33.4% B at 20 min, 90% B at 21 min, 90% B at 24 min, 20% B at 25 min, and 20% B at 40 min. For LC systems 4 and 5, solvent A was 5 mM ammonium acetate in water, and solvent B was 5 mM ammonium acetate in acetonitrile/water (98:2, v/v). The linear gradient for LC system 4 was as follows: 1% B at 0 min, 18% B at 30 min, 95% B at 31 min, 95% B at 34 min, 1% B at 35 min, and 1% B at 50 min. For LC system 5, solvent A was 20 mM potassium phosphate buffer (pH 7.4)/acetonitrile (98:2, v/v), and solvent B was acetonitrile/20 mM potassium phosphate buffer (pH 7.4) (70:30, v/v). The linear gradient was as follows: 20% B at 0 min, 20% B at 2 min, 30% B at 15 min, 40% B at 17 min, 42.5% B at 30

dx.doi.org/10.1021/tx500332y | Chem. Res. Toxicol. 2015, 28, 59−70

min, 90% B at 31 min, 90% B at 34 min, 20% B at 35 min, and 20% B at 50 min.

Mass Spectrometry. A TSQ-7000 triple quadrupole mass spectrometer (Thermo Fisher Scientific Inc., Waltham, MA) equipped with an ESI source was used in positive ion mode. The TSQ-7000 operating conditions were as follows: heated capillary temperature at 330 °C, and the nitrogen sheath gas and auxiliary gas pressures were 90 psi and 30 (arbitrary units), respectively. Full scanning analyses were performed in the range of m/z 300−1500. Argon was used as the collision gas in collision-induced dissociation experiments, coupled with MS/MS at 2.5−2.7 mTorr in the second (rf-only) quadrupole. Unit resolution was maintained for full-scan and MS/MS analyses. Matrix-assisted laser desorption ionization/time-of-flight (MALDI/TOF)-MS and MALDI/postsource decay (PSD) TOF-MS experiments were carried out using a Voyager-DE STR MALDI-TOF mass spectrometer (Applied Biosystems Inc., Foster City, CA) in positive ion mode with an accelerating voltage of 20 kV. The mass spectrometer was equipped with a nitrogen laser (337 nm) and had an ion path of 200 cm for linear mode and 300 cm for reflectron mode. All spectra presented were acquired in delayed extraction (extraction delay time: 100 ns) and reflectron modes with an average of 100−150 laser shots. TOF-MS experiments were performed in the mass range of m/z 100−3000. For PSD TOF-MS experiments, the mass window for the precursor ion selection was ca. ± 10 Da. Calibration was performed with four or five internal calibrants from the following: monoisotopic masses of the matrix monomer at m/z 190.0504, the matrix dimer at m/z 379.0930, Ang II (1−4) at m/z 552.2776, the matrix trimer at m/z 568.1400, Ang II at m/z 1046.5418, and Ang I at m/z 1296.6800. For MALDI/PSD TOF-MS analyses, PSD fragments were calibrated using monoisotopic masses of fragment ions generated from Ang II ($[M + H]^+$ at m/z 1046.5418, $[M + H]^+ - NH_3$ at m/z 1029.5152, y_7 at m/z 931.5148, $b_7 + H_2O$ at m/z 899.4734, b_6 at m/z 784.4100, a_6 at m/z 756.4151, b_5 at m/z 647.3511, a_5 at m/z 619.3562, $b_4 - NH_3$ at m/z 517.2405, y_3 at m/z 400.1979, $b_3 - NH_3$ at m/z 354.1772, and y_2 at m/z 263.1390).

Preparation and FT-IR Analysis of Ang C. Ang C was synthesized and supplied by Toray Research Center, Inc. The synthetic procedure was as follows: First, Fmoc-R(Pbf)VY(*t*Bu)IH-(Trt)PF-Resin (Fmoc, 9-fluorenylmethyloxycarbonyl; Pbf, 2,2,4,6,7-pentamethyldihydrobenzofuran-5-sulfonyl; *t*Bu, *tert*-butyl; Trt, trityl) was prepared by a typical solid-phase method using Fmoc-Arg(Pbf)-OH, Fmoc-Val-OH, Fmoc-Tyr(*t*Bu)-OH, Fmoc-Ile-OH, Fmoc-His-(Trt)-OH, Fmoc-Pro-OH, and Fmoc-Phe-OH. The following cyclization procedure was not provided because of a patent related issue. However, it can be easily assumed that the deprotection of the Fmoc group was followed by the insertion of C═O using triphosgene between the N-terminal amino group and the adjacent amide nitrogen.[30] FT-IR analysis of authentic Ang C exhibited an in-phase $(C{=}O)_2$ stretching vibration ($\nu_{ip}(C{=}O)_2$) at 1714 cm^{-1} and an out-of-phase $(C{=}O)_2$ stretching vibration ($\nu_{op}(C{=}O)_2$) at 1645 cm^{-1}, which results from the coupling of two carbonyl groups at the N-terminus. This is the typical C═O stretching pattern observed in five-membered cyclic imides such as hydantoins.[31] FT-IR spectra of Ang C, 5-methyl hydantoin ($\nu_{ip}(C{=}O)_2$, 1716 cm^{-1}; $\nu_{op}(C{=}O)_2$, 1684 cm^{-1}), Ang P (ν(C═O), 1636 cm^{-1}), Ang II (ν(C═O), 1636 cm^{-1}), and Ang III (ν(C═O), 1636 cm^{-1}) are shown in Supporting Information (Figure S1−S5, Supporting Information). When compared with the $\nu_{op}(C{=}O)_2$ of 5-methyl hydantoin (Figure S2, Supporting Information), the $\nu_{op}(C{=}O)_2$ band of Ang C (Figure S1, Supporting Information) was more intense, broader, and observed at a lower wavenumber because it was merged with the ν(C═O) band that arose from peptide bond (amide carbonyl group) vibrations. Ang P exhibited the ν(C═O) band at 1636 cm^{-1} with a small shoulder at 1662 cm^{-1} derived from the coupling of vicinal carbonyl groups in the N-terminus (Figure S3, Supporting Information). In the case of Ang II and Ang III, a single ν(C═O) band for peptide bond vibrations was observed at 1636 cm^{-1} in the 1600−1700 cm^{-1} region (Figure S4 and S5, Supporting Information, respectively).

Reaction of Ang II with ONE. A solution of ONE (300 μM) in 6 μL of methyl acetate/ethanol (1:1, v/v) was added to Ang II (100 μM) in 294 μL of 50 mM Chelex-treated PB (pH 7.4). The reaction mixture was incubated for 24 h at 37 °C. For time course experiments, a portion of the sample (10 μL) was withdrawn at various time points and added to 20 μL of internal standard (IS; Ang IV, 50 μM) in 50 mM Chelex-treated PB/acetonitrile (4:1, v/v). LC/ESI-MS analysis (10 μL) was conducted using LC system 1.

Reaction of Ang II with Cu(II)/AA. A solution of $CuSO_4{\cdot}5H_2O$ (5 or 10 μM) was added to Ang II (100 μM) in 50 mM Chelex-treated PB. The reaction was initiated by adding AA (50 or 100 μM) and continued for 24 h at 37 °C. For time course experiments, a portion of the sample (10 μL) was withdrawn at various time points and added to 20 μL of IS (Ang IV, 50 μM) in 50 mM Chelex-treated PB/acetonitrile (4:1, v/v). LC/ESI-MS analysis (10 μL) was conducted using LC system 1.

Reaction of Ang II with Zn(II)/AA, Fe(II)/AA, or Fe(III)/AA. A solution of each transition metal ion ($ZnSO_4{\cdot}7H_2O$, $FeSO_4{\cdot}7H_2O$, and $FeCl_3{\cdot}6H_2O$: 10 μM) was added to Ang II (100 μM) in 50 mM Chelex-treated PB. The reaction was initiated by adding 100 μM AA, and the mixture was incubated for 24 h at 37 °C. A portion of the sample (10 μL) was analyzed by LC/ESI-MS using LC system 1.

Sodium Borohydride Reduction of Ang C. Ang C was isolated by LC-UV (225 nm) using LC system 5 from the reaction of Ang II with Cu(II)/AA as described above. Retention times of Ang P and Ang C on LC system 5 were 12.8 and 14.2 min, respectively. Sodium borohydride reduction of Ang C was carried out as described previously.[27]

MALDI/TOF-MS and MALDI/PSD TOF-MS Analyses of Ang C. Ang C before or after sodium borohydride reduction was purified and desalted chromatographically on Oasis HLB (1 mL, 10 mg) cartridges. The cartridges were conditioned with acetonitrile (1 mL) followed by 0.1% aqueous trifluoroacetic acid (1 mL). The fraction containing Ang C (200 μL) was loaded on the cartridges and washed with 0.1% aqueous trifluoroacetic acid (200 μL × 3). Ang C was then recovered by elution with acetonitrile/water (6:4, v/v) containing 0.1% trifluoroacetic acid (200 μL × 2) and evaporated to dryness under nitrogen. The samples were redissolved in acetonitrile/water (1:1, v/v; 20 μL). Aliquots (0.5 μL) were loaded onto MALDI sample plates followed by matrix solution (0.5 μL, saturated CHCA in acetonitrile/water (1:1, v/v) containing 0.1% trifluoroacetic acid and 1−2 μM of internal calibrants) and allowed to dry at room temperature for MALDI/TOF-MS analysis.

Reaction of Ang P with Cu(II)/AA. A solution of $CuSO_4{\cdot}5H_2O$ (2 μM) was added to Ang P (20 μM) in 50 mM Chelex-treated PB. The reaction was initiated by adding AA (20 μM) and continued for 24 h at 37 °C. A portion of the sample (10 μL) was withdrawn at various time points and added to IS (20 μL, Ang IV, 50 μM) in 50 mM Chelex-treated PB/acetonitrile (4:1, v/v). LC/ESI-MS analysis (10 μL) was conducted using LC system 1.

Reaction of Ang P with Cu(II), Zn(II), Fe(II), or Fe(III). A solution of each transition metal ion ($CuSO_4{\cdot}5H_2O$, $ZnSO_4{\cdot}7H_2O$, $FeSO_4{\cdot}7H_2O$, and $FeCl_3{\cdot}6H_2O$: 2 μM) was added to a solution of Ang P (20 μM). The reaction mixture was incubated for 24 h at 37 °C. A portion of the sample (10 μL) was analyzed by LC/ESI-MS using LC system 1.

UV Irradiation of Ang II or Ang P in the Presence of Hydrogen Peroxide. A solution of Ang II or Ang P (100 μM) in 50 mM Chelex-treated PB was placed in a quartz cuvette and irradiated for 24 h in the presence of hydrogen peroxide (0, 0.1, 1.0 mM) with UVA using a PL-S 9W UV−A light source (Philips, Aachen, Germany) at a dose rate of approximately 4.5 mW/cm^2. The UVA lamp delivered UV light in the range of 315−380 nm with a peak at 370 nm. A portion of sample was withdrawn after 0, 8, 12, and 24 h of irradiation and analyzed (10 μL) by LC/ESI-MS using LC system 1.

APA-Mediated Metabolism of Ang Peptides. The enzyme assay was conducted by modification of a previously published method.[32] Ang II, Ang P, or Ang C (2 μM) was incubated with APA (0.2 μg/mL) at 37 °C in 25 mM Tris/HCl buffer (pH 7.5) containing 50 mM NaCl in the presence of 1 mM $CaCl_2$. The reaction was terminated after 20 min of incubation by adding 2.5% (v/v) formic

dx.doi.org/10.1021/tx500332y | Chem. Res. Toxicol. 2015, 28, 59−70

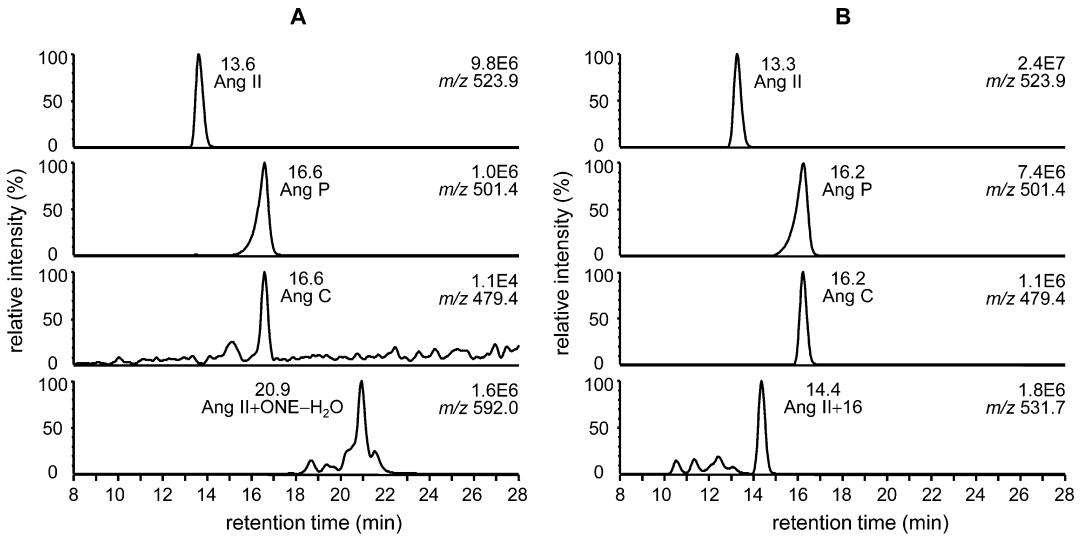

Figure 1. LC/ESI-MS analyses of the reactions of Ang II (100 μM) with (A) ONE (300 μM) or (B) Cu(II)/AA (10 or 100 μM) at 37 °C for 24 h.

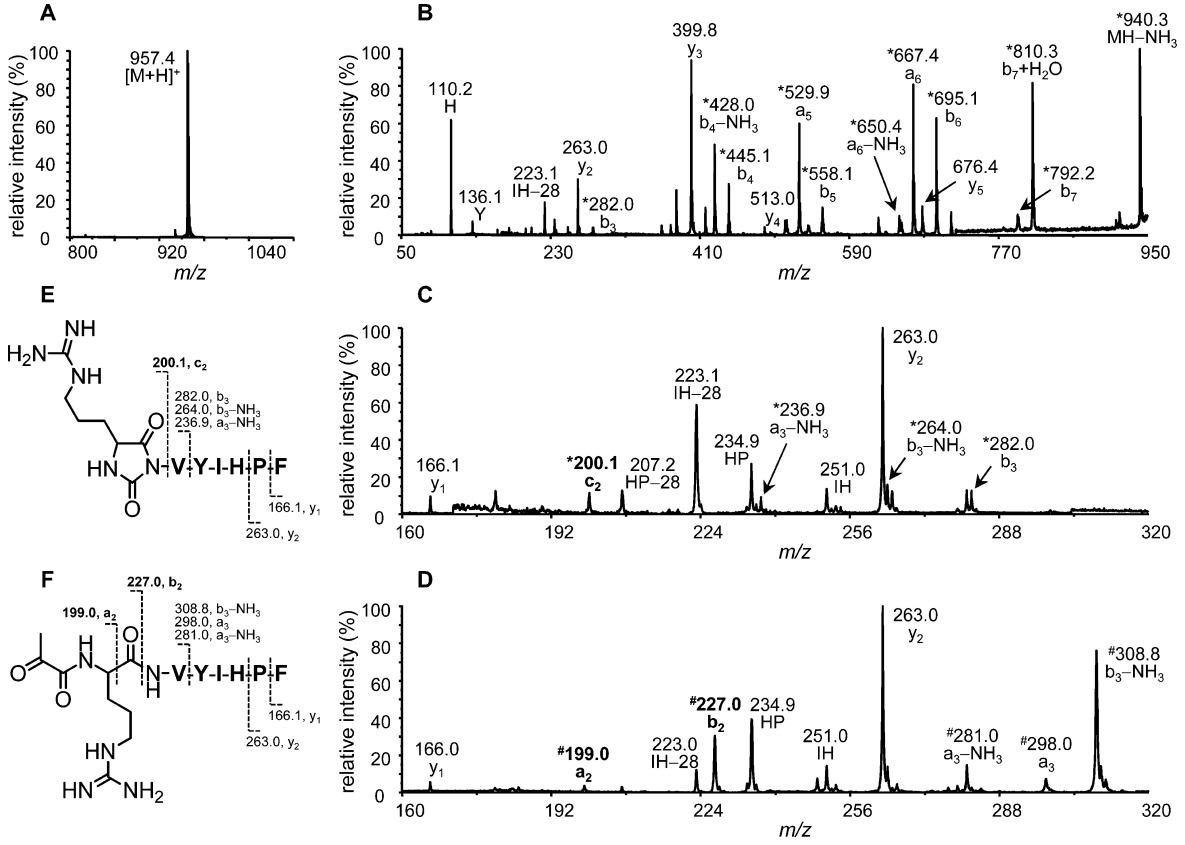

Figure 2. (A) MALDI/TOF-MS analysis of Ang C. (B) MALDI/PSD TOF-MS analysis of Ang C ($[M + H]^+$ at m/z 957.4) with a mass range of m/z 50−950 and (C) m/z 160−320. (D) MALDI/PSD TOF-MS analysis of Ang P ($[M + H]^+$ at m/z 1001.4) with a mass range of m/z 160−320. (E) Structure of Ang C with PSD product ions observed in C. (F) Structure of Ang P with PSD product ions observed in D. *Modified ion (− 89 Da). #Modified ion (− 45 Da). The m/z value on each peak is the observed monoisotopic mass.

acid (5 μL). A portion of the reaction mixture (10 μL) was analyzed by LC/ESI-MS using LC system 2.

Reaction of ONE with Other Bioactive Peptides. A solution of ONE (300 μM) in methyl acetate/ethanol (1:1, v/v; 6 μL) was added to each of the bioactive peptides (Ang A, Ang III, Ang IV, and Aβ_{1-11}: 100 μM) in 50 mM Chelex-treated PB (294 μL). The reaction mixture was incubated for 24 h at 37 °C. A portion of the sample (10 μL) at various time points was analyzed after dilution with acetonitrile (1:1, v/v) by LC/ESI-MS using LC system 3 for Ang A, Ang III, and Ang IV; LC system 4 for Aβ_{1-11}.

Reaction of Other Bioactive Peptides with Cu(II)/AA. A solution of $CuSO_4 \cdot 5H_2O$ (10 μM) was added to each of the bioactive peptides (Ang A, Ang III, Ang IV, and Aβ_{1-11}: 100 μM) in 50 mM Chelex-treated PB. The reaction was initiated by adding AA (100 μM) and continued for 24 h at 37 °C. A portion of the sample (10 μL) at various time points was analyzed after dilution with acetonitrile (1:1,

dx.doi.org/10.1021/tx500332y | Chem. Res. Toxicol. 2015, 28, 59−70

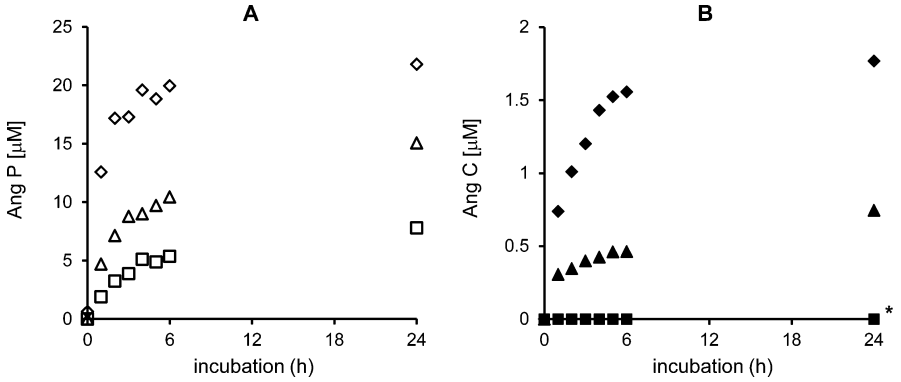

Figure 3. Formation of (A) Ang P (open symbols) and (B) Ang C (closed symbols) in the reaction of Ang II (100 μM) with ONE (300 μM, squares) or Cu(II)/AA (5 or 50 μM, triangles; 10 or 100 μM, diamonds) at 37 °C in 24 h. *Below the quantitation limit.

v/v) by LC/ESI-MS using LC system 3 for Ang A, Ang III, and Ang IV; and LC system 4 for Aβ_{1-11}.

RESULTS

LC/ESI-MS Analyses for Reactions of Ang II with ONE or Cu(II)/AA. LC/ESI-MS analysis of the reaction between Ang II and ONE at 37 °C for 24 h (Figure 1A) revealed the presence of Ang P at a retention time (t_R) of 16.6 min, ONE-modified Ang II (Ang II + ONE − H_2O) at t_R = 20.9 min, and residual Ang II at t_R = 13.6 min. A trace amount of Ang C was also detected at 16.6 min. The ESI mass spectrum of Ang P showed an expected $[M + H]^+$ ion at m/z 1001.5 ($[M + 2H]^{2+}$ = m/z 501.4), corresponding to a loss of 45 Da from Ang II ($[M + H]^+$ = m/z 1046.5; $[M + 2H]^{2+}$ = m/z 523.9). Ang II + ONE − H_2O showed an $[M + H]^+$ ion at m/z 1182.6 ($[M + 2H]^{2+}$ = m/z 592.0) corresponding to an increase in mass of 136 Da from Ang II. The MS/MS analysis of m/z 592.0 revealed that the modification occurred on Arg[2], as reported previously.[24] LC/ESI-MS analysis of the reaction between Ang II and Cu(II)/AA at 37 °C for 24 h (Figure 1B) showed increased production of Ang P and Ang C compared with the ONE reaction. In particular, the formation of Ang C was approximately 100 times higher in the Cu(II)/AA reaction. Ang C had an $[M + H]^+$ ion at m/z 957.4 ($[M + 2H]^{2+}$ = m/z 479.4), which corresponded to a loss of 89 Da from Ang II. The peak for oxidized Ang II (Ang II + 16) was observed at 14.4 min with an $[M + H]^+$ ion at m/z 1062.5 ($[M + 2H]^{2+}$ = m/z 531.7), and the MS/MS spectrum revealed that the oxidation occurred on His[6] (data not shown).

MALDI/TOF-MS and MALDI/PSD TOF-MS Analysis of Ang C before and after Sodium Borohydride Reduction. Ang C isolated from the reaction of Ang II with Cu(II)/AA showed an $[M + H]^+$ ion at m/z 957.4 (Figure 2A). The MALDI/PSD TOF-MS analysis of m/z 957.4 revealed that a modification occurred at the N-terminus (Figure 2B). All of the a, b, and c ions that were detected (c_2, a_3−a_6, and b_3−b_7) appeared with a loss of 89 Da. However, all of the y ions (y_1−y_5) remained unmodified, and the y_6 and y_7 ions were not detected. The PSD spectra of Ang II or Ang P clearly exhibited y_6 at m/z 775.4 and y_7 at m/z 931.5,[27] suggesting that modifications on Ang C could involve Arg[2] as well as Asp[1]. This possibility was further supported by the PSD spectra of Ang C and Ang P in the low mass region. The PSD spectrum of Ang C (Figure 2C) showed the presence of the c_2 ion at m/z 200.1, but not the a_2 or b_2 ions, which were observed in the PSD spectrum of Ang P (Figure 2D). On the basis of these results, the N-terminus of Ang C was expected to have the cyclic structure shown in Figure 2E. LC/ESI-MS and MALDI/TOF-MS analyses of an authentic Ang C showed that its LC and MS properties were identical to those of Ang C isolated from the reaction of Ang II with Cu(II)/AA. Ang C was then subjected to the sodium borohydride reduction. After the reaction, the product was further purified and desalted by solid-phase extraction, as described in the Materials and Methods section. MALDI-TOF/MS analysis revealed that Ang C was recovered intact after the reaction with sodium borohydride.

Formation of Ang P and Ang C from Reactions of Ang II with ONE or Cu(II)/AA. The formation of Ang P and Ang C was quantified in the reactions of Ang II (100 μM) with ONE (300 μM) or Cu(II)/AA (5/50 μM or 10/100 μM) for 24 h. Ang IV ($[M + H]^+$ = m/z 775.4, $[M + 2H]^{2+}$ = m/z 388.3, t_R = 14.3 min on LC system 1) was added as an IS to each time point sample prior to LC/ESI-MS analysis. Each standard solution containing IS was prepared using authentic Ang P and Ang C. Calibration curves were obtained by linear regression analysis of the MS peak area (in the extracted ion chromatogram of $[M + 2H]^{2+}$) ratios of the analytes to the IS. The concentrations of Ang P and Ang C were calculated by interpolation from the regression lines. In the reaction of Ang II with ONE, the formation of Ang P increased steadily during the incubation and reached its maximum level after 24 h, when the concentration was 7.8 μM (Figure 3A, open squares). Similar patterns were observed for the formation of Ang P in the Cu(II)/AA reactions. However, the level of Ang P at each time point was approximately 2-fold higher in the 5/50 μM reaction (open triangles) and 3-fold higher in the 10/100 μM reaction (open diamonds) than those in the ONE reaction. Thus, the Ang P concentrations after 24 h incubation were 15.1 and 21.8 μM, respectively. The formation of Ang C was also observed both in the ONE and Cu(II)/AA reactions. In the ONE reaction, Ang C at all of the time points was below the limit of quantitation of our current method (Figure 3B, closed squares). In contrast, quantifiable amounts of Ang C were produced in the Cu(II)/AA reactions. Patterns for the formation of Ang C were similar to those of Ang P. Its levels after 24 h of incubation were 0.8 and 1.8 μM in the 5/50 and 10/100 μM Cu(II)/AA reactions, respectively. The formation of Ang P and Ang C was also observed in the reaction of Ang II with other transition metal ions (Zn(II), Fe(II), and Fe(III)) in the presence of AA. However, the levels of Ang P and Ang C were lower by a factor of 30 or 50 compared with those produced in the Cu(II)/AA reaction.

dx.doi.org/10.1021/tx500332y | Chem. Res. Toxicol. 2015, 28, 59−70

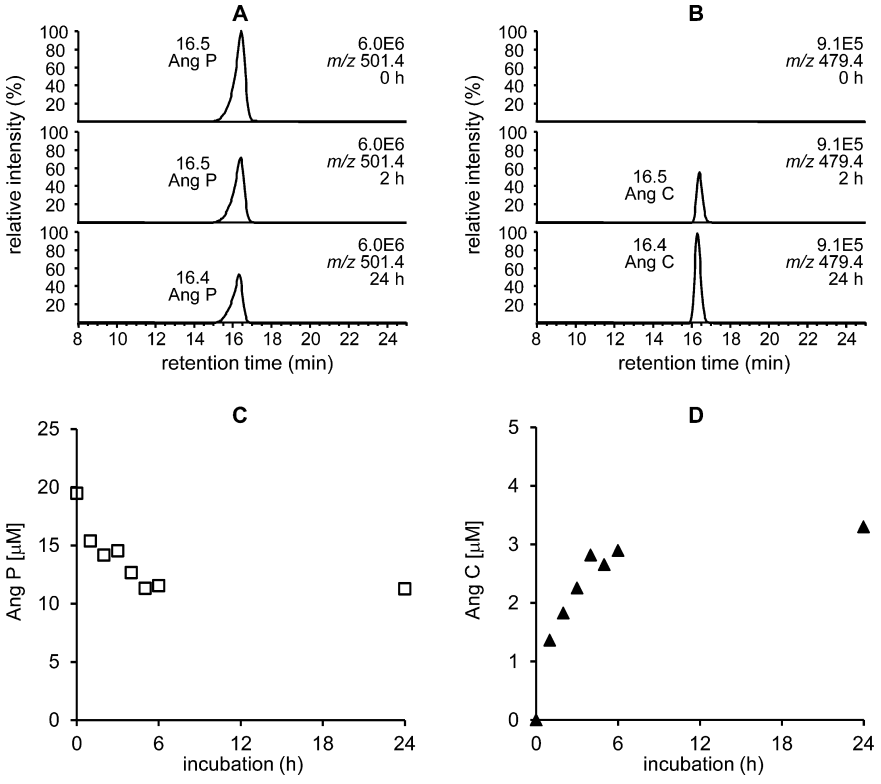

Figure 4. Conversion of Ang P (20 μM) to Ang C in the presence of Cu(II)/AA (2 or 20 μM) at 37 °C. LC/ESI-MS analyses of (A) Ang P and (B) Ang C at 0, 2, and 24 h. (C) Decomposition of Ang P and (D) formation of Ang C over 24 h.

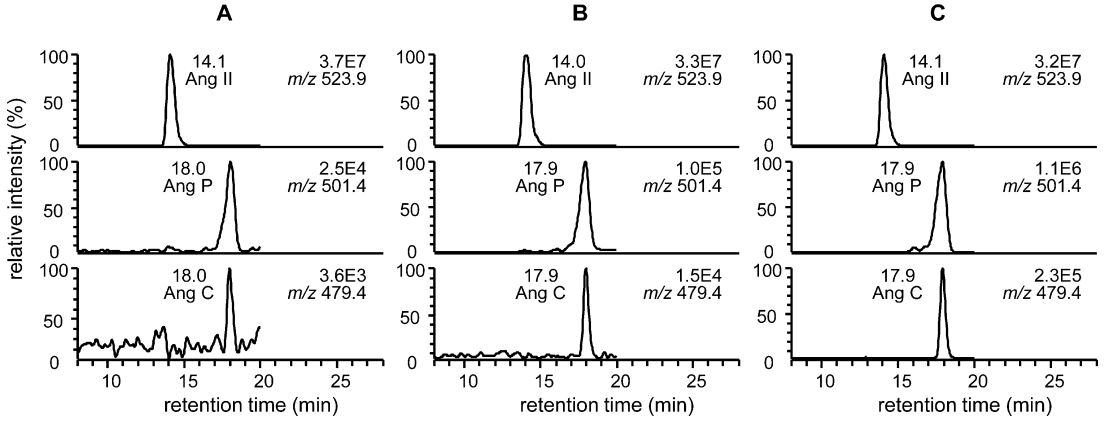

Figure 5. LC/ESI-MS analyses of Ang II (100 μM) in 50 mM Chelex-treated PB after UV irradiation for (A) 8 h, (B) 24 h, and (C) 24 h in the presence of hydrogen peroxide (1 mM).

Formation of Ang C from the Reaction of Ang P with Cu(II)/AA. To confirm the identity of the Ang C precursor, Ang P was incubated with Cu(II)/AA at 37 °C. Because 21.8 μM of Ang P was produced from the reaction of Ang II (100 μM) with Cu(II)/AA (10/100 μM) (Figure 3A), concentrations of 20 and 2/20 μM were used for Ang P and Cu(II)/AA, respectively. During the 24 h incubation, the intensity of the signal derived from Ang P was reduced by approximately 50% (Figure 4A). There was a concomitant increase in the formation of Ang C (Figure 4B). Levels of Ang P and Ang C at each time point were quantified as described above. The initial concentration of Ang P was calculated to be 19.5 μM, which was reduced to 15.4 μM after 1 h and 11.3 μM after 24 h of incubation (Figure 4C, open squares). Ang C was not detected at the beginning of the reaction. The Ang C peak was observed as a major product after 1 h of incubation, and the concentration of Ang C was 1.4 μM. The formation of Ang C increased gradually and reached a maximum of 3.3 μM after 24 h of incubation (Figure 4D, closed triangles). In addition to Ang C, trace amounts of Ang III, oxidized Ang P (Ang P + 16), and oxidized Ang C (Ang C + 16) were also detected in the reaction mixture after 24 h of incubation. When Ang P was incubated with Cu(II) alone for 24 h, a peak for Ang C was observed, although it was under our quantitation limit. Reactions with other transition metal ions (Zn(II), Fe(II), and Fe(III)) did not produce Ang C during the 24 h incubation. These results indicate that the formation of Ang C from Ang P is mediated by the hydroxyl radical.

Formation of Ang P and Ang C from UV Irradiation of Ang II or Ang P in the Presence of Hydrogen Peroxide.

dx.doi.org/10.1021/tx500332y | Chem. Res. Toxicol. 2015, 28, 59−70

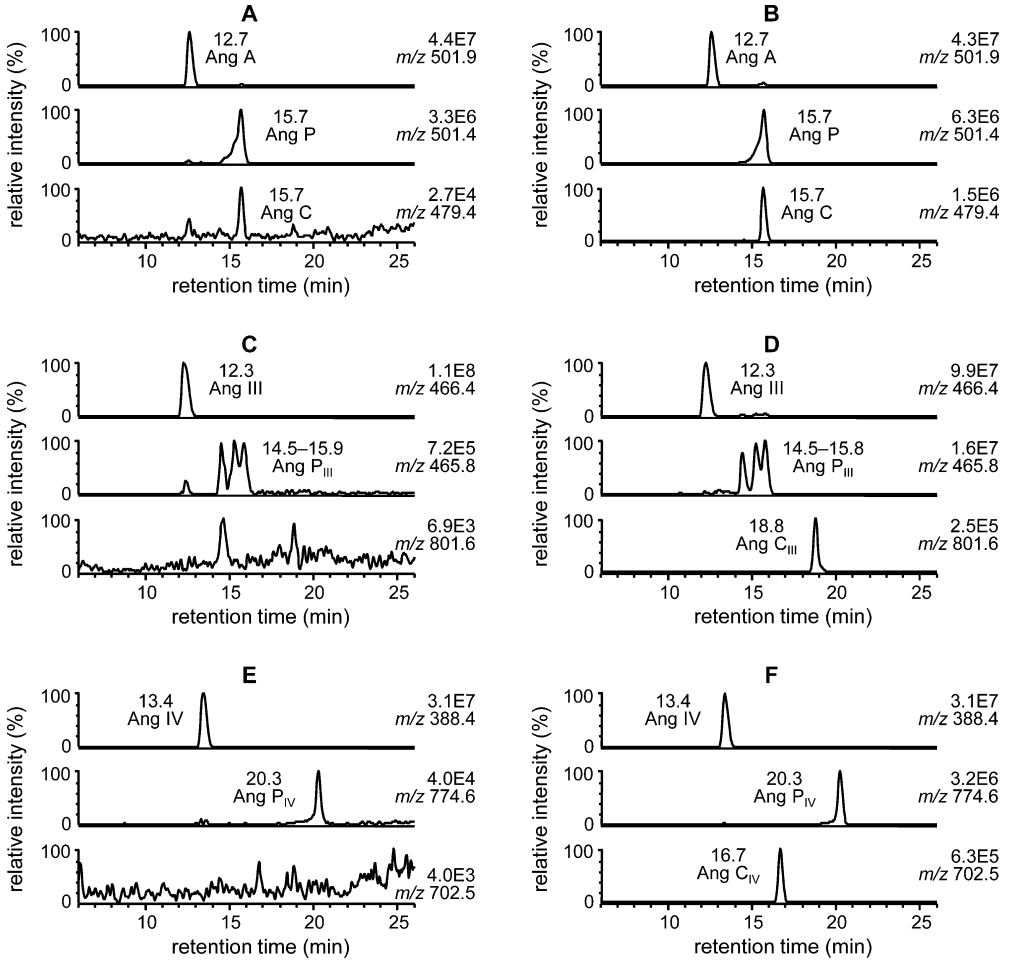

Figure 6. LC/ESI-MS analyses of the reactions between (A) Ang A (100 μM) and ONE (300 μM) or (B) Cu(II)/AA (10 or 100 μM), (C) Ang III (100 μM) and ONE (300 μM) or (D) Cu(II)/AA (10 or 100 μM), (E) Ang IV (100 μM) and ONE (300 μM) or (F) Cu(II)/AA (10 or 100 μM) at 37 °C for 24 h.

LC/ESI-MS analysis of the Ang II solution after 8 h of UV irradiation revealed the presence of Ang P (t_R = 18.0 min) and Ang C (t_R = 18.0 min) (Figure 5A). The formations of Ang P and Ang C increased during irradiation and reached their maximum levels after 24 h (Figure 5B). The levels of Ang P and Ang C increased further when Ang II was irradiated in the presence of hydrogen peroxide as a source of hydroxyl radical (Figure 5C). A similar result was observed for the conversion of Ang P to Ang C during irradiation.

LC/ESI-MS Analyses for Reactions of Ang peptides with ONE or Cu(II)/AA. LC/ESI-MS analysis of the reaction between Ang peptides (Ang A, Ang III, and Ang IV) and ONE at 37 °C for 24 h (Figure 6A, C, and E) detected their N-terminal α-ketoamide form at 15.7 min (Ang P from Ang A, Figure 6A middle), 14.5−15.9 min (Ang P_{III} from Ang III, Figure 6C middle), and 20.3 min (Ang P_{IV} from Ang IV, Figure 6E middle). As for the N-terminal cyclized form, only the Ang A reaction produced a trace amount of Ang C at 15.7 min (Figure 6A bottom). The ESI mass spectra of Ang P, Ang P_{III}, and Ang P_{IV} showed the expected $[M + H]^+$ ions at m/z 1001.5, 930.5, and 774.4 ($[M + 2H]^{2+} = m/z$ 501.4, 465.8, and 387.8), respectively, corresponding to a loss of 1 Da from their parent compounds, as reported previously.[24] The levels of Ang C, Ang C_{III}, and Ang C_{IV}, as well as N-terminal α-ketoamide Ang peptides were significantly increased in the reaction with Cu(II)/AA (Figure 6B, D, and F). In particular, the formation of Ang C_{III} (t_R = 18.8 min, Figure 6D bottom) and Ang C_{IV} (t_R = 16.7 min, Figure 6F bottom) was observed in only the Cu(II)/AA reaction. Ang C, Ang C_{III}, and Ang C_{IV} had expected $[M + H]^+$ ions at m/z 957.4, 801.6, and 702.5 ($[M + 2H]^{2+} = m/z$ 479.4, 401.2, and 351.7), which corresponded to a loss of 45 Da from Ang A, Ang III, and Ang IV, respectively.

APA-Mediated Metabolism of Ang Peptides. Ang II is a well-known substrate of the enzyme APA.[32] When Ang II (t_R = 16.5 min) was incubated in the assay buffer without APA for 20 min, it was recovered intact (Figure 7A, top). In the presence of APA and Ca(II) ions, Ang II was metabolized effectively, which led to a 62% conversion of Ang II to Ang III (t_R = 14.0 min, Figure 7A, bottom) within 20 min. A marginal amount of further degradation to Ang IV (t_R = 17.3 min, Figure 7A, bottom) was also observed. We then examined whether Ang P (t_R = 25.9 min) or Ang C (t_R = 26.2 min) could be a substrate of APA. Neither Ang P nor Ang C was cleaved by APA in our current assay system (Figure 7B and C). Modifying assay conditions, such as the amounts of APA and Ca(II) ions, and the incubation time, did not enhance the APA-mediated metabolism of Ang P or Ang C.

LC/ESI-MS and MS/MS Analyses for Reactions of $A\beta_{1-11}$ with ONE or Cu(II)/AA. LC/ESI-MS analysis of the reaction between $A\beta_{1-11}$ and ONE at 37 °C for 24 h (Figure 8A) revealed the presence of pyruvamide-$A\beta_{1-11}$ ($A\beta_{1-11}$-P, t_R = 23.7 min) with residual $A\beta_{1-11}$ (t_R = 17.5 min). No peak for

dx.doi.org/10.1021/tx500332y | Chem. Res. Toxicol. 2015, 28, 59−70

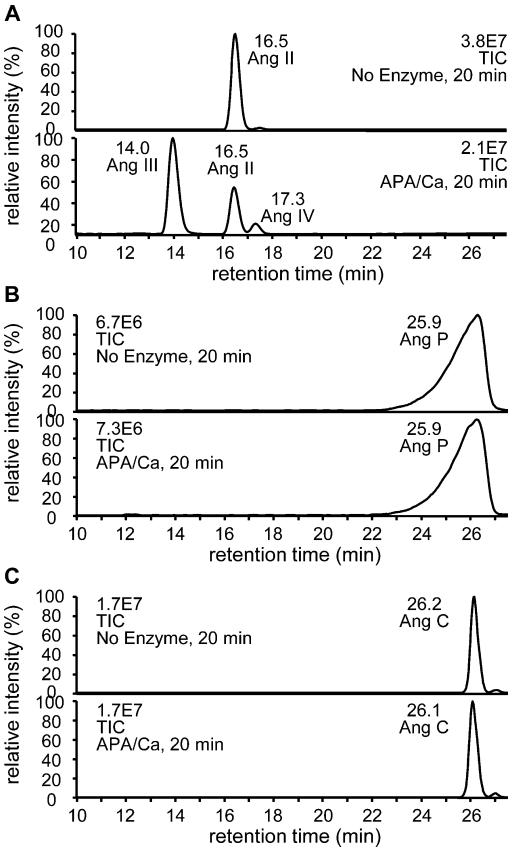

Figure 7. APA (20 ng)-mediated metabolism of (A) Ang II (2 μM), (B) Ang P (2 μM), and (C) Ang C (2 μM) in the presence of Ca (1 mM) at 37 °C for 20 min.

cyclized Aβ_{1-11}-P (Aβ_{1-11}-C) was observed. The ESI mass spectrum of Aβ_{1-11}-P showed the expected $[M + H]^+$ ion at m/z 1280.5 ($[M + 2H]^{2+} = m/z$ 640.8), corresponding to a loss of 45 Da from Aβ_{1-11} ($[M + H]^+ = m/z$ 1325.5, $[M + 2H]^{2+} = m/z$ 663.2). LC/ESI-MS analysis of the reaction between Aβ_{1-11} and Cu(II)/AA at 37 °C for 24 h (Figure 8B) revealed the presence of Aβ_{1-11}-P and Aβ_{1-11}-C (t_R = 20.7 min). The MS intensity of Aβ_{1-11}-P formed in the Cu(II)/AA reaction was approximately 10 times higher than that in the ONE reaction. Aβ_{1-11}-C had an $[M + H]^+$ ion at m/z 1236.5 ($[M + 2H]^{2+} = m/z$ 618.6), which corresponded to a loss of 89 Da from Aβ_{1-11}. A single peak for Aβ_{1-11} + ONE − H_2O (t_R = 22.4 min) and multiple peaks for oxidized Aβ_{1-11} (Aβ_{1-11} + 16, t_R = 14.2−17.6 min) were also detected in the ONE and Cu(II)/AA reactions, respectively. However, they appeared as minor products. LC/ESI-MS/MS analysis of Aβ_{1-11}-P at m/z 640.8 revealed that a modification occurred at the N-terminus (Figure 8C). All of the a and b ions that were detected (a_{10}, b_3, b_5, and b_7−b_{10}) appeared with a loss of 45 Da compared with that of Aβ_{1-11}. However, all of the y ions (y_1, y_2, and y_5) remained unmodified. The MS/MS spectrum of Aβ_{1-11}-C showed that the a_6, a_{10}, b_3, b_5, b_6, and b_3−b_{10} ions lost 89 Da from Aβ_{1-11} and that the y_1 and y_2 ions were unmodified, suggesting that a modification occurred at the N-terminus of Aβ_{1-11} (Figure 8D). Unlike Ang P and Ang C, neither the a_2 (m/z 114.1) and b_2 (m/z 142.1) ions of Aβ_{1-11}-P nor the c_2 (m/z 115.1) ion of Aβ_{1-11}-C were detected. It might be because of the lower ionization efficiency of Ala (the second amino acid of Aβ_{1-11}) when compared with that of Arg (the second amino acid of Ang II). Aβ_{1-11}-P and Aβ_{1-11}-C were then subjected to sodium borohydride reduction. LC/ESI-MS analyses of reduced Aβ_{1-11}-P revealed $[M + H]^+$ ions at m/z 1282.5 ($[M + 2H]^{2+} = m/z$ 641.8), which corresponded to the addition of two hydrogen atoms. Subsequent MS/MS analyses confirmed that the hydrogen atoms were added to the N-terminal pyruvamide moiety of Aβ_{1-11}-P. However, Aβ_{1-11}-C did not gain any hydrogen atoms upon reaction with sodium borohydride.

Formation of Aβ_{1-11}-P and Aβ_{1-11}-C from a Reaction of Aβ_{1-11} with ONE or Cu(II)/AA. The formation of Aβ_{1-11}-P and Aβ_{1-11}-C in the reaction of Aβ_{1-11} (100 μM) with ONE (300 μM) or Cu(II)/AA (10/100 μM) was plotted for 24 h using the MS peak intensity in the extracted ion chromatogram of $[M + 2H]^{2+}$. In the reaction of Aβ_{1-11} with ONE, the formation of Aβ_{1-11}-P was observed from the earliest time point (1 h) and increased during the incubation, reaching its maximum level after 24 h (Figure 9A, open squares). The MS peak intensity of the Aβ_{1-11}-P formed in the Cu(II)/AA reaction (Figure 9A, open diamonds) was approximately 10 to 60 times greater at each time point than that for the ONE reaction, although its formation pattern over 24 h was similar to that observed for the ONE reaction. The formation of Aβ_{1-11}-C was not observed in the reaction of Aβ_{1-11} with ONE (Figure 9B, closed squares). However, the peak for Aβ_{1-11}-C was detected from the beginning of the Cu(II)/AA reaction (Figure 9B, closed diamonds). After 24 h of incubation, its MS peak intensity was approximately 10% greater than that of Aβ_{1-11}-P.

DISCUSSION

In nature, α-ketoamide moieties are found in bioactive marine metabolites, such as cyclotheonamides,[33] orbiculamide A,[34] and keramamides.[35] Cyclotheonamide A belongs to an unusual class of serine protease inhibitor, and its α-ketoamide group is responsible for binding to the active site.[36] Recently, α-ketoamide peptides have been identified as inhibitors of serine and cysteine proteases. Cellular targets that are inhibited by α-ketoamides include thrombin, a serine protease that converts fibrinogen to fibrin,[37] and caspase, a cysteine protease that plays a role in apoptosis.[38] α-Ketoamides have also been successfully used as a core structure for the inhibition of HIV-1 protease.[39] The postulated mechanism for inhibition is based on the covalent interaction of α-ketoamide moieties with nucleophilic residues of the active site, which is stabilized by the electron-withdrawing effect of the second carbonyl group.[36] N-Terminal α-ketoamide (pyruvamide) was unexpectedly identified during studies of peptide-cleaving catalyst drug candidates selective for target proteins. Upon incubation with Co(III) cyclen compounds, Ang I and Ang II were cleaved by oxidative decarboxylation instead of peptide hydrolysis; the N-terminal Asp residues were converted to pyruvate residues.[40] In a separate study of the site-specific modification of the peptide N-terminus, pyridoxal 5′-phosphate was shown to convert Ang I to pyruvamide-Ang I.[41]

ONE can also mediate the formation of N-terminal α-ketoamide on Ang peptides containing not only N-terminal Asp[27] but also other amino acid residues, such as Ala, Arg, and Val.[28] The initial reaction of the α-amino group on Ang peptides occurs at C-1 of ONE and yields a Schiff base intermediate. It exists in equilibrium with its tautomers and undergoes hydrolysis to form the ketone moiety at the N-terminus of Ang peptides (α-ketoamide-Ang peptides) (Scheme 1A). α-Ketoamide peptides were formed more

dx.doi.org/10.1021/tx500332y | Chem. Res. Toxicol. 2015, 28, 59−70

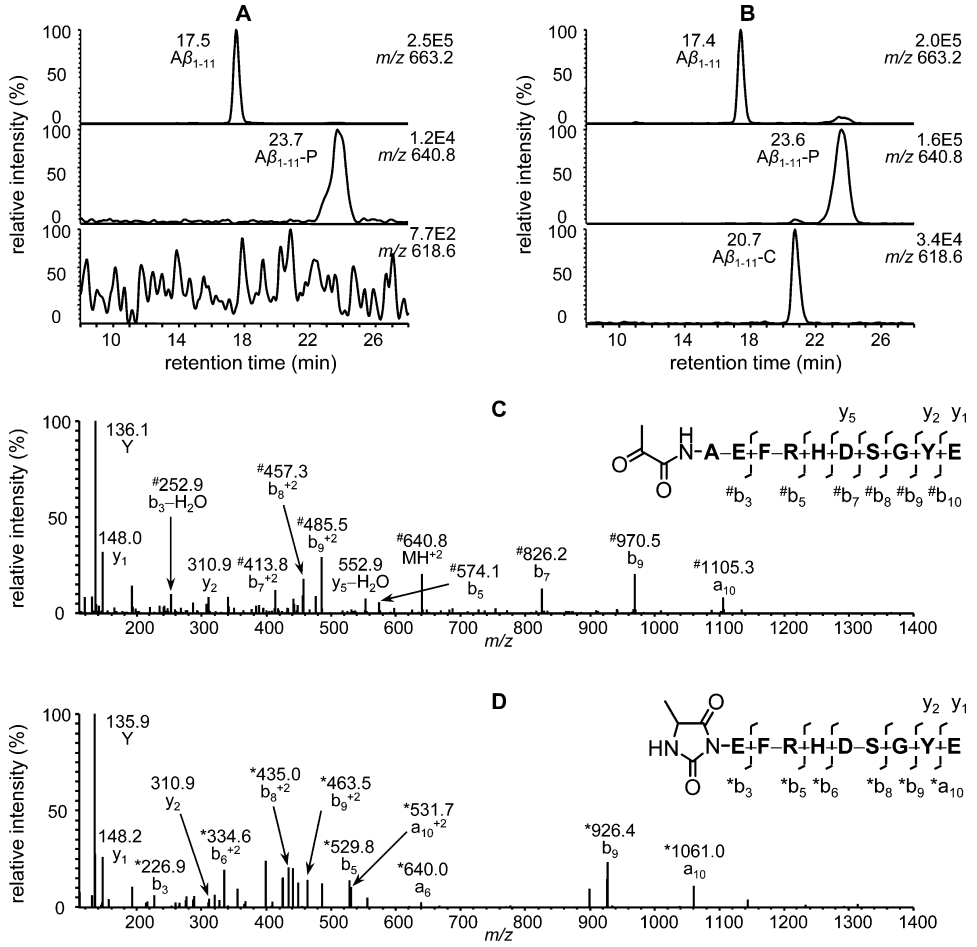

Figure 8. LC/ESI-MS analyses of the reaction between Aβ_{1-11} (100 μM) and (A) ONE (300 μM) or (B) Cu(II)/AA (10 or 100 μM) at 37 °C for 24 h. LC-ESI/MS/MS (collision energy = 55%) analyses of (C) Aβ_{1-11}-P ($[M + 2H]^{2+}$ at m/z 640.8) and (D) Aβ_{1-11}-C ($[M + 2H]^{2+}$ at m/z 618.6).

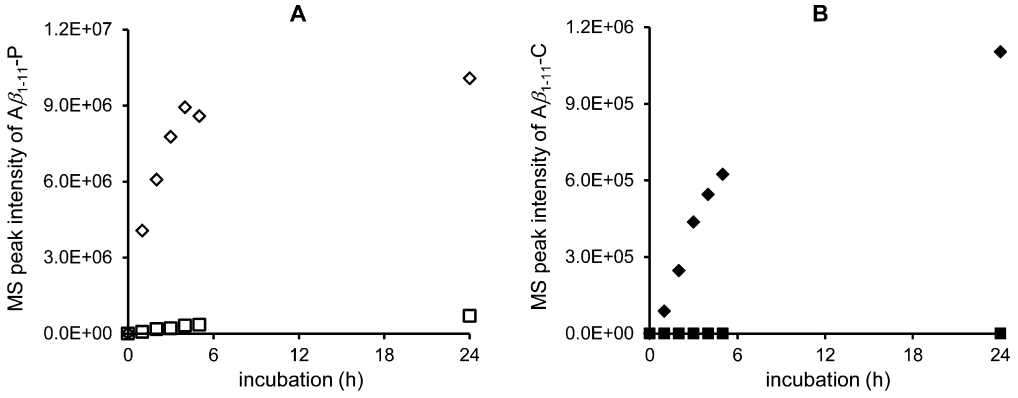

Figure 9. Formation of (A) Aβ_{1-11}-P (open symbols) and (B) Aβ_{1-11}-C (closed symbols) in the reaction of Aβ_{1-11} (100 μM) with ONE (300 μM; squares) or Cu(II)/AA (10 or 100 μM, diamonds) at 37 °C in 24 h.

efficiently in the reaction with the hydroxyl radical.[28] The reaction is initiated by the hydroxyl radical-dependent abstraction of the N-terminal α-hydrogen atom. In the presence of oxygen, the carbon-centered radical is rapidly converted to the peroxyl radical. The loss of $HO_2^{\bullet}$ followed by hydrolysis of the ketimine intermediate yields α-ketoamide-Ang peptides (Scheme 1B). The resulting N-terminal α-ketoamides were then converted to D- and L-Ang peptides by nonenzymatic transamination in the presence of PM (Scheme 1C).[28] In this study, we demonstrate that N-terminal α-ketoamide peptides can be cyclized by the reaction with the hydroxyl radical generated from the Cu(II)/AA system (Scheme 1D). The reaction of Ang II with Cu(II)/AA resulted in the formation of Ang C with an $[M + H]^+$ ion at m/z 957.4 ($[M + 2H]^{2+} = m/z$ 479.4), corresponding to a loss of 89 Da from Ang II. The modification site at the N-terminus was revealed by MALDI/PSD TOF-MS analyses, showing that all of the a, b, and c ions (−89 Da) were modified and that all of the y ions were intact. The PSD spectrum exhibited a c_2 ion but not a_2, b_2, y_6, or y_7 ions, which provides good evidence for the N-terminal

dx.doi.org/10.1021/tx500332y | Chem. Res. Toxicol. 2015, 28, 59−70

Scheme 1. Proposed Mechanisms for the (A) ONE- and (B) Hydroxyl Radical-Mediated Formation of α-Ketoamide-Ang Peptides[a]

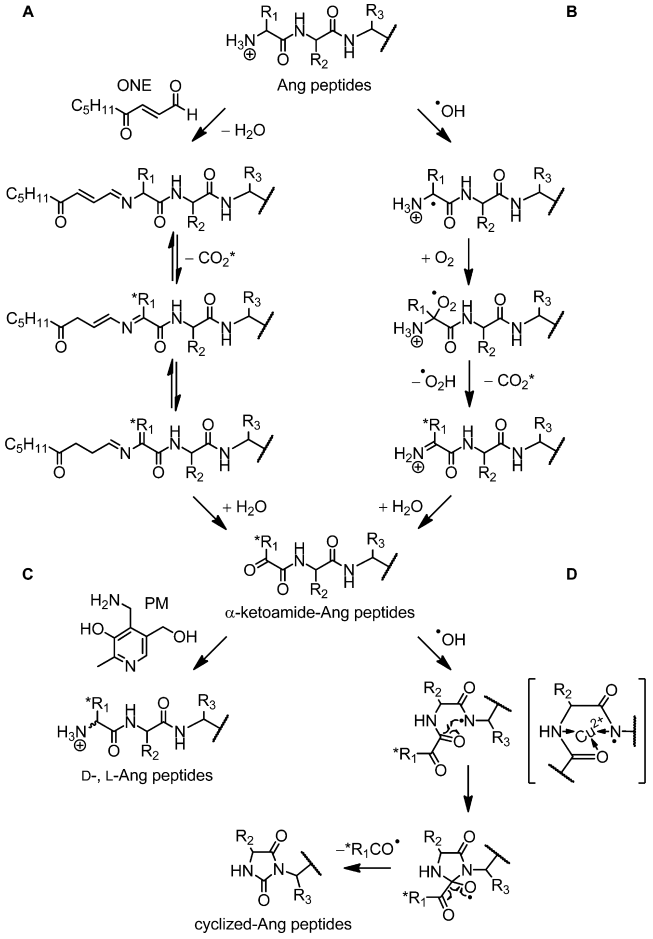

[a]Conversion of α-ketoamide-Ang peptides to (C) D-,L-Ang peptides in the presence of PM and (D) cyclized-Ang peptides by the hydroxyl radical generated from the Cu(II)/AA system. The structure in brackets indicates the possible stabilization of the aminyl radical by coordination to the Cu(II) ion. *Decarboxylation occurs only when R_1 = Asp.

cyclization, including Asp[1] and Arg[2] residues (Figure 2). The structure of Ang C was further confirmed by comparison with the authentic standard, where the presence of five-membered cyclic imide in the N-terminus was supported by IR spectroscopy (Figure S1–S5, Supporting Information). Ang P was one of the major products in the reaction between Ang II and ONE, although the Cu(II)/AA reaction produced Ang P more efficiently by converting approximately 22% of Ang II (Figure 3A). However, Ang C was generated almost exclusively in the Cu(II)/AA reaction (Figure 3B), indicating that the hydroxyl radical mediated the cyclization reaction. Ang P was then incubated in the presence of Cu(II)/AA to confirm the direct precursor of Ang C. After 24 h, Ang C was observed as the single major product, and its concentration corresponded to approximately 17% conversion of Ang P (Figure 4). When other transition metal ions (Zn(II), Fe(II), and Fe(III)) with or without AA were used in the reactions, only a trace amount or no Ang C was observed. N-Terminal cyclization also occurred on other Ang peptides containing N-terminal Ala, Arg, and Val (Figure 6). Similar to the Ang II reactions, N-terminal cyclized-Ang peptides were formed almost exclusively in the Cu(II)/AA reaction. On the basis of these results, we propose a mechanism that involves the formation of a nitrogen-centered (aminyl) radical (Scheme 1D). The aminyl radical is stabilized by chelation to Cu(II) ions and adds an amide carbonyl double bond in the vicinity, which forms a five-membered ring containing an alkoxy radical. The following β-scission reaction of the alkoxyl radical results in the cleavage of the terminal R_1CO group. It is unusual that the hydroxyl radical-mediated hydrogen abstraction occurs at the N-terminal α-carbon (to form Ang P) or at R_3 α-carbon (to form Ang C). To confirm the involvement of Cu(II) in those radical reactions, UV and hydrogen peroxide were employed as a hydroxyl radical generating system. UV irradiation of Ang II in the presence of hydrogen peroxide produced substantial amounts of Ang P and Ang C (Figure 5). A significant level of Ang P was also converted to Ang C by treatment with UV and hydrogen peroxide. These results indicate that the free hydroxyl radical can medicate the formation of Ang P and Ang C from Ang II and Ang P, respectively. The higher yields of Ang P and Ang C in Cu(II)/AA system suggests that Cu(II) leads to more site-specific generation of the hydroxyl radical by chelation effect.

The AT_1 receptor mediates most of the physiological effects of Ang II on the cardiovascular, endocrine, and neuronal systems.[42] In our previous study, we developed an MS-based label-free binding assay for the AT_1 receptor to test the biological effects of modified Ang II.[29] The K_d value for Ang II was calculated as 0.96 ± 0.16 nM. The well-known AT_1 receptor antagonist, losartan, had a K_i of 19 nM. Our competition-binding assay showed that the affinity of Ang P (K_i = 42 nM) for the AT_1 receptor was much lower than that of Ang II and that the affinity of Ang C (K_i = 2600 nM) was even lower than that of Ang P. These results indicated that the N-terminal α-ketoamide group and particularly its cyclized form significantly inhibit binding to the AT_1 receptor. Ang II is further metabolized to Ang III through the cleavage of the N-terminal Asp residue by APA, which is present in the blood, kidneys, and brain.[32] Recent studies provide evidence for the involvement of APA-mediated Ang II metabolism in the control of blood pressure.[43,44] In our APA assay system, Ang II was converted to Ang III in 20 min (Figure 7A). However, neither Ang P nor Ang C was a substrate for APA in various assay conditions (Figure 7B and C), suggesting that oxidative modifications of Ang II to Ang P or Ang C can affect its metabolism in vivo.

$A\beta_{1-11}$-P was formed in the reaction of $A\beta_{1-11}$ with ONE or Cu(II)/AA (Figure 8A and B, middle) as reported previously.[28] It was converted to D-$A\beta_{1-11}$-A and L-$A\beta_{1-11}$-A in the presence of PM.[28] Hydroxyl radicals generated from the Cu(II)/AA system produced 10 times more $A\beta_{1-11}$-P than ONE and mediated further cyclization of $A\beta_{1-11}$-P to form $A\beta_{1-11}$-C (Figure 8B bottom). The structures of $A\beta_{1-11}$-P and $A\beta_{1-11}$-C were confirmed by LC/ESI-MS and MS/MS analyses before and after the sodium borohydride reduction. The patterns of their formation during the 24 h incubation were similar to those for the formation of Ang P and Ang C. We are currently examining the possible effects of N-terminal α-ketoamide formation and its cyclization on the self-aggregation of various Aβ peptides.

In summary, we have demonstrated that the hydroxyl radical can mediate N-terminal cyclization of peptides through the formation of α-ketoamides. N-Terminal α-ketoamide peptides can be formed by the reaction with ONE or a hydroxyl radical.

dx.doi.org/10.1021/tx500332y | Chem. Res. Toxicol. 2015, 28, 59–70

However, cyclization of N-terminal α-ketoamide occurred almost exclusively in the presence of Cu(II)/AA, which is one of the most efficient hydroxyl radical generating systems.[45,46] For Ang II, the hydroxyl radical mediated a 22% conversion of Ang II to Ang P and a 17% conversion of Ang P to Ang C. The cyclized N-terminus and the α-ketoamide significantly modified the biological functions of the peptide. Thus, the affinities of Ang P and Ang C toward the AT_1 receptor were much lower than that of Ang II. In addition, Ang P and Ang C were not metabolized further by APA. Our current studies are now focused on examining the effects of these N-terminal modifications on other bioactive peptides and detecting them in biological systems.

■ ASSOCIATED CONTENT

Supporting Information

FT-IR spectra of Ang C, 5-methyl hydantion, Ang P, Ang II, and Ang III. This material is available free of charge via the Internet at http://pubs.acs.org.

■ AUTHOR INFORMATION

Corresponding Authors

*(S.H.L.) Tel: +81-22-795-6817. Fax: +81-22-795-6816. E-mail: sh-lee@mail.pharm.tohoku.ac.jp,
*(T.O.) E-mail: t-oe@mail.pharm.tohoku.ac.jp.

Funding

This work was supported in part by a Grant-in-Aid for Challenging Exploratory Research (to T.O., 21659035 for 2009−2010) and Grants-in-Aid for Scientific Research (C) (to S.H.L., 25460186 for 2013−2015; to T.G., 40344684 for 2012−2014) from the Japan Society for the Promotion of Science (JSPS).

Notes

The authors declare no competing financial interest.

■ ACKNOWLEDGMENTS

We thank Professor Ian A. Blair (University of Pennsylvania, Philadelphia, PA) for kindly donating the parts for TSQ-7000, and Ryo Satoh, M.S. (Tohoku University) for help with conducting IR spectroscopy.

■ ABBREVIATIONS

AA, L-ascorbic acid; $A\beta_{1-11}$, amyloid beta 1−11; D-$A\beta_{1-11}$-A, D-Ala^1-L-Ala^2-L-Glu^3-L-Phe^4-L-Arg^5-L-His^6-L-Asp^7-L-Ser^8-L-Gly^9-L-Tyr^{10}-L-Glu^{11}; L-$A\beta_{1-11}$-A, L-Ala^1-L-Ala^2-L-Glu^3-L-Phe^4-L-Arg^5-L-His^6-L-Asp^7-L-Ser^8-L-Gly^9-L-Tyr^{10}-L-Glu^{11}; $A\beta_{1-11}$-P, pyruvamide-$A\beta_{1-11}$; $A\beta_{1-11}$-C, cyclized $A\beta_{1-11}$-P; Ang, angiotensin; Ang P, pyruvamide-Ang II; Ang P_{III}, α-ketoamide-Ang III; Ang P_{IV}, α-ketoamide-Ang IV; Ang C, N-terminal cyclized-Ang II; Ang C_{III}, N-terminal cyclized-Ang III; Ang C_{IV}, N-terminal cyclized-Ang IV; APA, aminopeptidase A; AT_1, angiotensin II type 1; CHCA, α-cyano-4-hydroxycinamic acid; ESI, electrospray ionization; Fmoc, 9-fluorenylmethyloxycarbonyl; HNE, 4-hydroxy-2(*E*)-nonenal; IS, internal standard; LC, liquid chromatography; MALDI/TOF-MS, matrix-assisted laser desorption ionization/time-of-flight-mass spectrometry; $[M + H]^+$, protonated molecule; MS/MS, tandem mass spectrometry; ONE, 4-oxo-2(*E*)-nonenal; PB, phosphate buffer; Pbf, 2,2,4,6,7-pentamethyldihydrobenzofuran-5-sulfonyl; PM, pyridoxamine; PSD, postsource decay; ROS, reactive oxygen species; *t*Bu, *tert*-butyl; t_R, retention time; Trt, trityl

■ REFERENCES

(1) Halliwell, B. M., and Gutterige, J. M. C. (2007) *Free Radicals in Biology and Medicine*, 4th ed., Oxford University Press, New York.
(2) Lee, S. H., and Blair, I. A. (2001) Oxidative DNA damage and cardiovascular disease. *Trends Cardiovasc. Med. 11*, 148−155.
(3) Ames, B. N., Shigenaga, M. K., and Hagen, T. M. (1993) Oxidants, antioxidants, and the degenerative diseases of aging. *Proc. Natl. Acad. Sci. U.S.A. 90*, 7915−7922.
(4) Gonzalez, F. J. (2005) Role of cytochromes P450 in chemical toxicity and oxidative stress: studies with CYP2E1. *Mutat. Res. Mol. Mech. Mutagen. 569*, 101−110.
(5) Thannickal, V. J., and Fanburg, B. L. (2000) Reactive oxygen species in cell signaling. *Am. J. Physiol. Cell. Mol. Physiol. 279*, L1005−L1028.
(6) Finkel, T. (2011) Signal transduction by reactive oxygen species. *J. Cell Biol. 194*, 7−15.
(7) Grimsrud, P. A., Xie, H., Griffin, T. J., and Bernlohr, D. A. (2008) Oxidative stress and covalent modification of protein with bioactive aldehydes. *J. Biol. Chem. 283*, 21837−21841.
(8) Girotti, A. W. (1998) Lipid hydroperoxide generation, turnover, and effector action in biological systems. *J. Lipid Res. 39*, 1529−1542.
(9) Morelli, R., Russo-Volpe, S., Bruno, N., and Lo Scalzo, R. (2003) Fenton-dependent damage to carbohydrates: free radical scavenging activity of some simple sugars. *J. Agric. Food Chem. 51*, 7418−7425.
(10) Xu, G., and Chance, M. R. (2007) Hydroxyl radical-mediated modification of proteins as probes for structural proteomics. *Chem. Rev. 107*, 3514−3543.
(11) Hawkins, C. L., and Davies, M. J. (2001) Generation and propagation of radical reactions on proteins. *Biochim. Biophys. Acta 1504*, 196−219.
(12) Davies, M. J. (2005) The oxidative environment and protein damage. *Biochim. Biophys. Acta 1703*, 93−109.
(13) Schöneich, C. (2005) Methionine oxidation by reactive oxygen species: reaction mechanisms and relevance to Alzheimer's disease. *Biochim. Biophys. Acta 1703*, 111−119.
(14) Schöneich, C. (2008) Mechanisms of protein damage induced by cysteine thiyl radical formation. *Chem. Res. Toxicol. 21*, 1175−1179.
(15) Stadtman, E. R., and Levine, R. L. (2003) Free radical-mediated oxidation of free amino acids and amino acid residues in proteins. *Amino Acids 25*, 207−218.
(16) Stadtman, E. R. (1990) Metal ion-catalyzed oxidation of proteins: biochemical mechanism and biological consequences. *Free Radical Biol. Med. 9*, 315−325.
(17) Stadtman, E. R. (1993) Oxidation of free amino acids and amino acid residues in proteins by radiolysis and by metal-catalyzed reactions. *Annu. Rev. Biochem. 62*, 797−821.
(18) Dean, R., Fu, S., Stocker, R., and Davies, M. (1997) Biochemistry and pathology of radical-mediated protein oxidation. *Biochem. J. 324*, 1−18.
(19) Lee, S. H., Rindgen, D., Bible, R. H., Hajdu, E., and Blair, I. A. (2000) Characterization of 2′-deoxyadenosine adducts derived from 4-oxo-2-nonenal, a novel product of lipid peroxidation. *Chem. Res. Toxicol. 13*, 565−574.
(20) Pollack, M., Oe, T., Lee, S. H., Silva Elipe, M. V., Arison, B. H., and Blair, I. A. (2003) Characterization of 2′-deoxycytidine adducts derived from 4-oxo-2-nonenal, a novel lipid peroxidation product. *Chem. Res. Toxicol. 16*, 893−900.
(21) Zhu, P., Lee, S. H., Wehrli, S., and Blair, I. A. (2006) Characterization of a lipid hydroperoxide-derived RNA adduct in rat intestinal epithelial cells. *Chem. Res. Toxicol. 19*, 809−817.
(22) Oe, T., Lee, S. H., Silva Elipe, M. V., Arison, B. H., and Blair, I. A. (2003) A novel lipid hydroperoxide-derived modification to arginine. *Chem. Res. Toxicol. 16*, 1598−1605.
(23) Oe, T., Arora, J. S., Lee, S. H., and Blair, I. A. (2003) A novel lipid hydroperoxide-derived cyclic covalent modification to histone H4. *J. Biol. Chem. 278*, 42098−42105.
(24) Lee, S. H., Takahashi, R., Goto, T., and Oe, T. (2010) Mass spectrometric characterization of modifications to angiotensin II by

lipid peroxidation products, 4-oxo-2(*E*)-nonenal and 4-hydroxy-2(*E*)-nonenal. *Chem. Res. Toxicol. 23*, 1771−1785.
(25) Jian, W., Lee, S. H., Mesaros, C., Oe, T., Elipe, M. V. S., and Blair, I. A. (2007) A novel 4-oxo-2(*E*)-nonenal-derived endogenous thiadiazabicyclo glutathione adduct formed during cellular oxidative stress. *Chem. Res. Toxicol. 20*, 1008−1018.
(26) Kajita, R., Goto, T., Lee, S. H., and Oe, T. (2013) Aldehyde stress-mediated novel modification of proteins: epimerization of the N-terminal amino acid. *Chem. Res. Toxicol. 26*, 1926−1936.
(27) Lee, S. H., Goto, T., and Oe, T. (2008) A novel 4-oxo-2(*E*)-nonenal-derived modification to angiotensin II: oxidative decarboxylation of N-terminal aspartic acid. *Chem. Res. Toxicol. 21*, 2237−2244.
(28) Lee, S. H., Kyung, H., Yokota, R., Goto, T., and Oe, T. (2014) N-Terminal α-ketoamide peptides: formation and transamination. *Chem. Res. Toxicol. 27*, 637−648.
(29) Lee, S. H., Masuda, T., Goto, T., and Oe, T. (2013) MALDI-TOF/MS-based label-free binding assay for angiotensin II type 1 receptor: application for novel angiotensin peptides. *Anal. Biochem. 437*, 10−16.
(30) Zhang, D., Xing, X., and Cuny, G. D. (2006) Synthesis of hydantoins from enantiomerically pure α-amino amides without epimerization. *J. Org. Chem. 71*, 1750−1753.
(31) Nyquist, R. A., and Fiedler, S. L. (1995) Infrared study of five- and six-membered type cyclic imides. *Vib. Spectrosc. 8*, 365−386.
(32) Goto, Y., Hattori, A., Ishii, Y., Mizutani, S., and Tsujimoto, M. (2006) Enzymatic properties of human aminopeptidase A: regulation of its enzymatic activity by calcium and angiotensin IV. *J. Biol. Chem. 281*, 23503−23513.
(33) Fusetani, N., Matsunaga, S., Matsumoto, H., and Takebayashi, Y. (1990) Bioactive marine metabolites. 33. Cyclotheonamides, potent thrombin inhibitors, from a marine sponge *Theonella* sp. *J. Am. Chem. Soc. 112*, 7053−7054.
(34) Fusetani, N., Sugawara, T., Matsunaga, S., and Hirota, H. (1991) Orbiculamide A: a novel cytotoxic cyclic peptide from a marine sponge *Theonella* sp. *J. Am. Chem. Soc. 113*, 7811−7812.
(35) Kobayashi, J., Itagaki, F., Shigemori, H., Ishibashi, M., Takahashi, K., Ogura, M., Nagasawa, S., Nakamura, T., and Hirota, H. (1991) Keramamides B. apprx. D, novel peptides from the Okinawan marine sponge *Theonella* sp. *J. Am. Chem. Soc. 113*, 7812−7813.
(36) Maryanoff, B. E., Qiu, X., Padmanabhan, K. P., Tulinsky, A., Almond, H. R., Andrade-Gordon, P., Greco, M. N., Kauffman, J. A., Nicolaou, K. C., and Liu, A. (1993) Molecular basis for the inhibition of human alpha-thrombin by the macrocyclic peptide cyclotheonamide A. *Proc. Natl. Acad. Sci. U.S.A. 90*, 8048−8052.
(37) Boatman, P. D., Ogbu, C. O., Eguchi, M., Kim, H. O., Nakanishi, H., Cao, B., Shea, J. P., and Kahn, M. (1999) Secondary structure peptide mimetics: design, synthesis, and evaluation of beta-strand mimetic thrombin inhibitors. *J. Med. Chem. 42*, 1367−1375.
(38) Brady, K. D., Giegel, D. A., Grinnell, C., Lunney, E., Talanian, R. V., Wong, W., and Walker, N. (1999) A catalytic mechanism for caspase-1 and for bimodal inhibition of caspase-1 by activated aspartic ketones. *Bioorg. Med. Chem. 7*, 621−631.
(39) Sheha, M. M., Mahfouz, N. M., Hassan, H. Y., Youssef, A. F., Mimoto, T., and Kiso, Y. (2000) Synthesis of di- and tripeptide analogues containing alpha-ketoamide as a new core structure for inhibition of HIV-1 protease. *Eur. J. Med. Chem. 35*, 887−894.
(40) Kim, M., Jeon, J. W., and Suh, J. (2005) Angiotensin-cleaving catalysts: conversion of N-terminal aspartate to pyruvate through oxidative decarboxylation catalyzed by Co (III) cyclen. *J. Biol. Inorg. Chem. 10*, 364−372.
(41) Gilmore, J. M., Scheck, R. A., Esser-Kahn, A. P., Joshi, N. S., and Francis, M. B. (2006) N-terminal protein modification through a biomimetic transamination reaction. *Angew. Chem., Int. Ed. 45*, 5307−5311.
(42) Campbell, D. J. (1987) Circulating and tissue angiotensin systems. *J. Clin. Invest. 79*, 1−6.
(43) Mizutani, S., Ishii, M., Hattori, A., Nomura, S., Numaguchi, Y., Tsujimoto, M., Kobayshi, H., Murohara, T., and Wright, J. W. (2008) New insights into the importance of aminopeptidase A in hypertension. *Heart Failure Rev. 13*, 273−284.
(44) Ferreira, A. J., and Raizada, M. K. (2008) Aminopeptidase A: could it be a novel target for neurogenic hypertension? *Hypertension 51*, 1273−1274.
(45) Vidrio, E., Jung, H., and Anastasio, C. (2008) Generation of hydroxyl radicals from dissolved transition metals in surrogate lung fluid solutions. *Atmos. Environ. 42*, 4369−4379.
(46) Charrier, J. G., and Anastasio, C. (2011) Impacts of antioxidants on hydroxyl radical production from individual and mixed transition metals in a surrogate lung fluid. *Atmos. Environ. 45*, 7555−7562.